

UniMLVG: Unified Framework for Multi-view Long Video Generation with Comprehensive Control Capabilities for Autonomous Driving

Rui Chen ^{1*}, Zehuan Wu ^{2†}, Yichen Liu ², Yuxin Guo ², Jingcheng Ni ², Haifeng Xia ¹, Siyu Xia ¹
¹ School of Automation, Southeast University, China ² SenseTime Research
 {chenr, hfxia, xsy}@seu.edu.cn; {wuzehuan, liuyichen, guoyuxin, nijingcheng}@sensetime.com
 Demo & Code & Checkpoints: <https://sensetime-fvg.github.io/UniMLVG/>

Abstract

The creation of diverse and realistic driving scenarios has become essential to enhance perception and planning capabilities of the autonomous driving system. However, generating long-duration, surround-view consistent driving videos remains a significant challenge. To address this, we present UniMLVG, a unified framework designed to generate extended street multi-perspective videoscise control. By integrating single- and multi-view driving videos into the

training data, our approach updates cross-frame and cross-view modules across three stages with different training objectives, substantially boosting the diversity and quality of generated visual content. Additionally, we employ the explicit viewpoint modeling in multi-view video generation to effectively improve motion transition consistency. Capable of handling various input reference formats (e.g., text, images, or video), our UniMLVG generates high-quality multi-view videos according to the corresponding condition constraints such as 3D bounding boxes or frame-level text descriptions. Compared to the best models with similar capabilities, our framework achieves improvements of 21.4% in FID and 36.5% in FVD.

^{1*} Work during the internship in SenseTime.

^{2†} Corresponding authors.

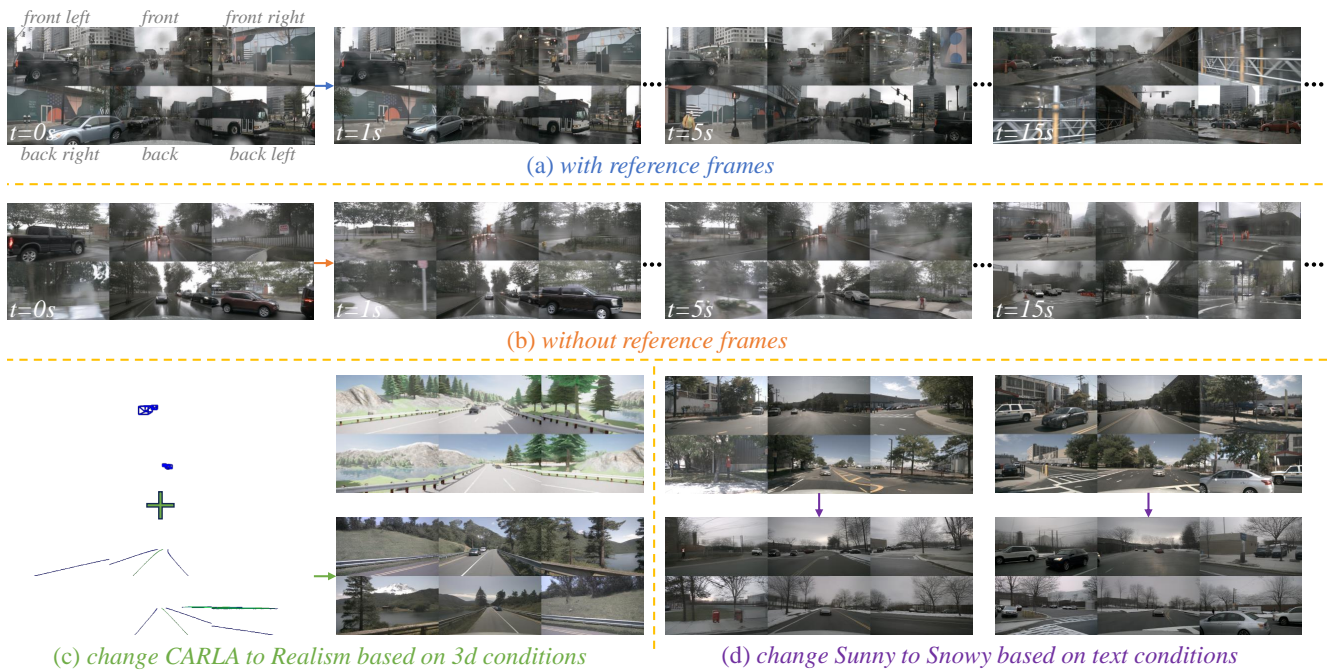


Figure 1. **Four tasks our model can perform:** (a) generating a 20s multi-view video based on reference frames; (b) generating a 20s multi-view video without any reference frames; (c) creating a realistic surround-view video from conditions obtained in a simulated environment; (d) altering weather conditions from sunny to snowy, driven by text-based prompts.

1. Introduction

Autonomous driving technology [21, 22, 60] is poised to transform human transportation and significantly enhance traffic safety. To achieve this, substantial data collection becomes necessary yet seriously increases both economic burden and labor costs. This situation motivates the exploration and adoption of simulation data. However, the disparity between simulated and real-world scenarios still obstructs practical application and perception algorithm. For this issue, generative artificial intelligence provides a promising solution by synthesizing high-quality traffic data [14, 50, 58]. Meanwhile, the recent studies [49, 62] have demonstrated that these synthetic driving videos effectively support safe vehicle maneuvering, bridging critical gaps in real-world readiness.

From these frontier explorations, the main demands of effective generated driving videos include long-term multi-view consistency, condition-based controllability, and diversity. However, existing generative algorithms fail to satisfy these requirements simultaneously. For instance, DriveGAN [24] and DriveDreamer [49] introduce action-based autoregressive techniques to generate next-frame driving images. But, they both overlook the importance of multi-view perspectives in autonomous driving, limiting their ability to generate comprehensive multi-view data. MagicDrive [12] addresses this by incorporating 3D control information and cross-view modules to create multi-view images. Although they leverage the approach [55] to produce videos, their outputs are short and lack temporal consistency. Recent efforts [23, 30, 50] focus on generating controllable, multi-view videos over longer sequences. However, due to the limitations of single-objective training and small-scale datasets, they struggle to achieve temporal consistency and diversity. Importantly, the aforementioned works depend on scene-level descriptions to generate corresponding videos without fine-grained text conditions.

To achieve further breakthroughs, this paper proposes a novel generative framework UniMLVG to obtain highly consistent and controllable multi-view videos. Built upon a DiT-based image generation model [10], UniMLVG incorporates temporal and cross-view modules to capture dynamic sequences and information across multiple viewpoints. To enhance consistency, the multi-task training objective constraints and explicit perspective modeling are considered in our method. For diversity of generated instances, over 1,000 hours driving scene data with single-view and multi-view formats is utilized for model training. In terms of multi-condition control, we integrate both 3D conditions—such as 3D bounding boxes and high-definition maps (HDmaps)—and image-wise textual descriptions. In addition, our UniMLVG effectively supports text-to-video (T2V), image-to-video (I2V), and video-to-video (V2V) generation by using a progressive training strategy and

demonstrates exceptional performance in both text-based and 3D condition-based editing, as shown in Fig. 1. In summary, the primary contributions involve:

- To simulate the practical traffic scenarios, a novel multi-task, multi-condition, multi-stage training strategy is developed into UniMLVG and improves training stability.
- Extensive empirical analyses reveal that leveraging multiple datasets and image-level descriptions significantly enhances the diversity and text-based controllability of generated videos across various weather and times.
- According to experimental results, our UniMLVG surpasses the existing street video generation techniques in temporal consistency and frame quality, especially in its capability to perform diverse generation tasks.

2. Related Works

2.1. Video Generation and Editing

Video generation and editing hold vital importance in various fields, particularly in autonomous driving. These technologies enable the creation and manipulation of realistic video content, which is crucial for improving the perception and planning of autonomous systems in diverse scenarios. Traditional methods for video generation widely adopt techniques including Autoencoder [8, 16, 19], Generative Adversarial Network (GAN) [7, 25, 39, 42, 47] and Autoregressive Model [41, 53, 54, 56]. However, these approaches often fail to create realistic and diverse video and are unable to precisely control the content through text or layout.

In recent years, the advancement of diffusion models has revolutionized the field of image and video generation. Integrating the aforementioned techniques into the diffusion models, diffusion-based approaches [1, 15, 18, 34, 44, 51, 59, 63, 65] has become the mainstream of video generation and editing, due to their ability to produce high-quality videos with comprehensive control capabilities. Furthermore, the promising results of large-scale generative models like [4, 32] have inspired researchers to use these models as real-world simulators, significantly influencing the field of driving simulation [20, 49, 57]. For instance, DriveDreamer [49] takes the reference frame, the road structural information and text description as input and employs three types of attention blocks within the diffusion mode to predict the future frames. GenAD [57] leverages a large scale of YouTube videos as data to pretrain data and divides the training process into two stages, allowing the model to progressively learn image and video denoising. Despite their success, these methods generate single-view videos, which are less useful compared to multi-view videos, as autonomous vehicles need to perceive the surroundings rather than just the front view information only.

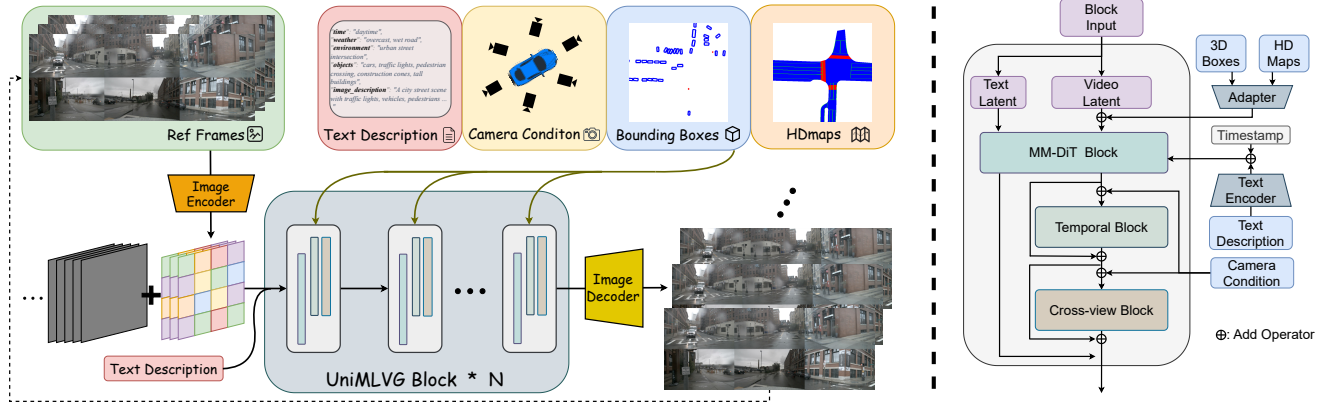


Figure 2. **Overall framework of the model.** *left*: The encoded reference frames are concatenated with the noise latent as video latent and fed into N UniMLVG blocks with the text latent. The diverse conditions including image-level descriptions, camera pose, and 3D conditions are injected into each UniMLGV block and interact with the video latent to guide the generated contents. Finally, the model outputs the subsequent frames, which can then be used as the reference frame for the next autoregressive generation. Note that our model can produce driving video based on those conditions only, where the reference frames are not required. *right*: Details of the UniMLVG block. A UniMLVG block comprises three distinct sub-blocks to perform attention across different dimensions, while the different conditions are integrated into the video latent in different positions during the forward passing.

2.2. Multi-view Video Generation

Compared to standard video generation, multi-view video generation remains relatively underexplored, due to the challenges in ensuring the consistency across perspectives and time series initial trials simply adopts the video diffusion architecture. For instance, MagicDrive [12] encodes high-level controls such as text and bounding boxes independently and flatten those conditions into an embedding sequence. In contrast, DreamForge [30] employs a trainable ControlNet [61] to fuse multi-modality condition. Drive-WM [50] generates videos from a few views using a diffusion model in the first stage and then utilizes multi-view factorization to predict additional views conditioned on the pre-generated ones. DiVE [23] leverages the DiT structure within its diffusion model and applies a view-inflated attention mechanism to compute attention across features from all viewpoints. Extending the design of [49], DriveDreamer-2 [62] concatenates all images per frame into a large single image, and only cross-frame modules are adopted in the forward pass. Despite these approaches, they usually rely on a reference frame to generate subsequent content and the quality of the videos significantly degrades as the sequence length increases. Additionally, they struggle to address inconsistencies across different views and timestamps. Based on the aforementioned issues, we introduce our unified model, which can provide precise control, generate high-quality videos and guarantee the spatial and temporal consistency.

3. Method

Fig. 2 illustrates the overall architecture of our proposed UniMLVG. Our method mainly enhances the DiT-based im-

age generation model [10] with two additional modules: the temporal module \mathcal{T} and the cross-view module \mathcal{C} . UniMLVG is capable of generating extended street-view videos and performing text-based and 3D-conditioned editing by using a multi-task, multi-condition, and multi-stage training strategy across diverse datasets. And, the integration of different street-view datasets (single/multi-view) with the corresponding modeled viewpoints is utilized to achieve the generation of consistent, long-duration multi-view videos.

3.1. Unified Framework

We choose the DiT-based model [10] as the backbone for image generation over alternatives like [3, 11, 32, 38] and extend the MM-DiT block, shown in the right of Figure 2 to our UniMLVG block to achieve an optimal balance of generation quality, scalability, model size, and flexibility in text-based control. For our diffusion model’s optimization, we employ the conditional rectified flows [10, 26, 27] loss as the primary objective.

$$\mathcal{L} = \mathbb{E}_{\epsilon \sim \mathcal{N}(0, I)} \left[\|v_{\theta}(z_t, t, c) - (z_0 - \epsilon)\|^2 \right],$$

where v is the model, θ is the parameters, t is the timestep and c is the condition.

The temporal and cross-view modules are positioned directly after the Multimodal Diffusion Transformer (MM-DiT) block to maintain consistency across time and viewpoints. Specifically, we apply the same self-attention module while adjusting input dimensions to suit the specific task. Given the noisy latent $z_t \in \mathbb{R}^{T \times V \times H \times W \times C}$, where T is the frame length and V represents the number of viewpoints, we adjust the attention sequence lengths differently for the temporal and cross-view modules. In the

temporal module, we flatten the dimensions VHW , resulting in a shape of $T \times (VHW) \times C$. In contrast, in the cross-view module, we combine THW , producing $V \times (THW) \times C$. Additionally, we use an absolute positional encoding method [46] that employs sine and cosine functions at varying frequencies to separately encode the positional information of both frames and viewpoints.

3.2. Multi-task

We observe that when using only the video prediction task, the quality of the generated video deteriorates significantly after a few autoregressive iterations. We believe this is due to the model’s excessive reliance on reference frames, which leads to accumulated autoregressive errors. To address this issue, we propose a multi-task training strategy to improve long-term video quality and coherence. Specifically, we design four training tasks: video prediction (VP), image prediction (IP), video generation (VG), and image generation (IG). In VP, we utilize the embeddings of the first k frames from n viewpoints as reference frames, setting their timestep to 0. In IP, we mask 50% of the reference frames, requiring the model to use the remaining discrete reference information to generate images at the masked positions. In VG, the model generates the next l frames of a multi-view video based solely on the given conditions, without any reference frames. In IG, we drop the temporal module to prevent the model from overly relying on temporal continuity, thus preserving its ability to maintain cross-view consistency. During training, these tasks are executed by sampling a mask $M \in \mathbb{R}^{T \times V}$ based on a predefined ratio, with the loss calculation excluding predictions of reference frames, as described below:

$$\mathcal{L} = \mathbb{E}_{\epsilon \sim \mathcal{N}(0, I)} \left[\|(1 - M) \odot (v_{\theta}(z_t, t, c) - (z_0 - \epsilon))\|^2 \right].$$

Additionally, our multi-task approach differs from that of DriveDreamer-2 [62] in several aspects. First, UniMLVG utilizes multiple reference frames to achieve more diverse combinations. Second, unlike DriveDreamer-2, which is limited to a forward-facing reference frame, UniMLVG randomly selects viewpoints in IP. Furthermore, we incorporate the IG task to enhance performance.

3.3. Multi-condition

To help the model grasp the physical dynamics of autonomous driving scenes, we introduce both local conditions (such as 3Dboxes and HDmaps) and global conditions (including view-specific text descriptions). Notably, we are the first to explicitly model camera parameters to incorporate perspective condition for this task.

Local Conditions. We unify local conditions as image-based conditions. Similar to the approach used in T2I-Adapter [31], we introduce a lightweight image adapter for

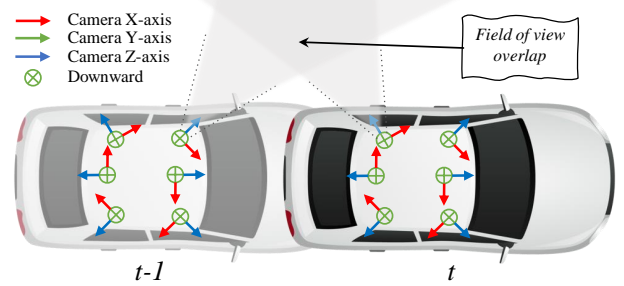


Figure 3. **Field of view overlap between cameras over time.** It can reduce the uncertainty in generating new scene frames.

efficient processing. By projecting 3Dboxes or HDmaps and mapping the instance identity to the color space, we generate sparse images $I_l \in \mathbb{R}^{T \times V \times H' \times W' \times 3}$, matching the original image size. These conditional images are concatenated and input into the adapter to obtain multi-level features $C_l \in \mathbb{R}^{k \times T \times V \times H \times W \times C}$, which are then added to the latent representation at the corresponding layer to integrate the conditional information.

Global Conditions. Building on the approach in [10], we utilize three text encoders [6, 36, 37] to extract multi-level textual features, which are managed through joint attention mechanisms and AdaLN [33] with latent variables. Notably, we use image-level descriptions instead of scene-level ones, enabling more customized content generation. In our method, the primary global condition is text, but the framework is also well-suited to incorporate additional information such as video frame rate and actions.

Perspective Modeling. Apparently, there exist overlaps in the image contents between the adjacent views at the same moment and between the same view at different time. Moreover, as shown in Figure 3, there is also a significant field of view overlap between the current viewpoint of the moving vehicle and one of previous viewpoint. All of these overlaps help to reduce the uncertainty in generating new scene images. Meanwhile, modeling camera poses explicitly has proven effective in recent works [13, 40] that generate multi-view images of static scenes. We believe this is also applicable for generating consistent dynamic driving scenes. Specifically, we set the optical center of the forward-facing camera in the first frame as the origin to establish a unified coordinate system for all viewpoints. The camera rays are encoded to produce ray features and subsequently added to the image latent representation. The formula for ray coordinate encoding is as follows, where j represents the encoding dimension (set to 8 in this paper), and p represents the coordinate value.

$$\text{Enc}(v) = MLP(\sin(2^0 \pi p), \cos(2^0 \pi p), \sin(2^1 \pi p), \cos(2^1 \pi p), \dots, \sin(2^{j-1} \pi p), \cos(2^{j-1} \pi p)).$$

Method	Multi-view	Video	Duration	FID↓	FVD↓	mAP _{obj} ↑	mIoU _{road} ↑	mIoU _{vehicle} ↑
Oracle	-	-	-	-	-	35.56	73.67	31.86
DriveGAN [24]	×	✓	3s	73.4	502.3	-	-	-
DriveDreamer [49]	×	✓	4s	52.6	452.0	-	-	-
MagicDrive [12]	✓	✓	5s	19.1	218.1	12.30	61.05	<u>27.01</u>
Drive-WM [50]	✓	✓	20s	15.2	122.7	20.66	<u>65.07</u>	-
DriveDreamer-2 [62]	✓	✓	7s	<u>11.2</u>	55.7	-	-	-
DreamForge [30]	✓	✓	20s	16.0	224.8	13.80	-	-
DiVE [23]	✓	✓	20s	-	94.6	24.55	-	-
Ours	✓	✓	20s	8.8	<u>60.1</u>	<u>22.50</u>	70.81	29.12

Table 1. Comparison of the generation quality and condition-following metrics on nuScenes validation set. ↑/↓ indicates that a higher/lower value is better. The best results are in **bold**, while the second best results are in underlined (when other methods are available).

3.4. Multi-stage

Our goal is to utilize a wide range of currently available datasets, including both single-view and multi-view street scene videos, to impart driving scene priors to the model. Considering that single-view and multi-view data differ in the number of viewpoints and annotation information, we implement a multi-stage training strategy to ensure stable and efficient model convergence.

Stage I. Empowering the model with the capability to anticipate future driving scenarios from a forward-facing perspective. We train \mathcal{T} on a substantial collection of publicly available forward-facing driving videos [57]. This dataset, notable for its large-scale, high-resolution and multi-scenario, helps the model generate temporal coherent frames. During this phase, we freeze the initial weights of SD3 [10] and bypass the cross-view modules.

Stage II. Infusing the model with the ability to generate from multiple viewpoints and effectively follow conditional inputs. We train \mathcal{C} using several multi-view datasets [5, 43, 52]. These datasets provide multi-view videos, camera calibration parameters, and 3D annotations, allowing the model to generate diverse multi-view videos. During this phase, only the temporal and cross-view modules are trained, while the backbone remains frozen.

Stage III. To further improve generation quality, we perform full fine-tuning in this phase. With the model’s generation capabilities well-developed from the first two stages, this phase typically requires a minimal number of training epochs. Therefore, this stage is optional.

4. Experiments

4.1. Experiment Details

Datasets. We use the single-view dataset OpenDV-Youtube [57] and the multi-view datasets nuScenes [5], Waymo [43], and Argoverse2 [52]. OpenDV-Youtube is exclusively used for pretraining, while nuScenes, Waymo, and Argoverse2 are divided into training and validation sets

following their original splits. The training duration totals 1,498 hours, comprising 1,486 hours from OpenDV-Youtube, 4.6 hours from nuScenes, 4.4 hours from Waymo, and 3.1 hours from Argoverse2. We leverage available dataset annotations, including 3Dboxes, HDmaps and camera parameters. Meanwhile, nuScenes with 12 Hz interpolated annotations [2] is used. Additionally, text descriptions for all frames and views are generated at 2 Hz using [48].

Evaluation Metrics. To assess the effectiveness of our method in terms of realism, continuity, and precise control, we selected four key metrics to compare against existing multi-view image and video generation methods. For realism, we use the widely recognized Fréchet Inception Distance (FID) [17]. To estimate temporal coherence in our videos, we measure consistency using Fréchet Video Distance (FVD) [45]. For a fair comparison, we conduct evaluation following [12], using 150 scenes from the nuScenes validation set, with 6 viewpoints per scene and 16 frames per viewpoint, totaling 900 videos for FVD computation. Additionally, we sample 10,000 images from these 900×16 frames to calculate FID. For controllability, we evaluate two perception tasks: 3D object detection [28] and BEV segmentation [64], following the approach MagicDrive [12].

Implement Details. We use 3 frames as reference for autoregressive prediction. A fixed learning rate of 8×10^{-5} is applied across all stages and optimized with AdamW [29]. The conditions dropping rate is set uniformly at 20%, and classifier-free guidance scale is 3. The inference steps set 50. All experiments are conducted on A800 GPUs.

4.2. Experiment Results

Quantitative Results. We report quantitative experimental metrics on the nuScenes validation set, as shown in Tab. 1. Overall, our model achieves quite promising results, with a significant improvement of 21.4% in FID compared to the second-best method. Firstly, this is attributed to the powerful text-to-image model [10] which is used as our backbone. Additionally, as demonstrated in the ablation



Figure 4. **Text-based weather editing at different times of day:** (a) shows text-based control changing sunny to rainy. (b) demonstrates text editing to generate a snowy night scenario. In each subfigure, the left side shows the ground truth, while the right side presents the generated results, with the top and bottom representing the front and rear viewpoints.

study 4.3, the multi-task and multi-stage training strategies make significant contributions. In terms of temporal consistency, we achieve a 36.5% improvement over DiVE [23], which also uses the DiT [18] architecture, and obtain the second place in FVD, slightly lower than DriveDreamer-2 [62]. However, DriveDreamer-2 can only produce 7s video while UniMLVG can generate longer video up to 20s, almost three times as longer as DriveDreamer-2. Additionally, unlike DriveDreamer-2 [62], UniMLVG does not stitch multiple views into a single image for generation, which reduces memory usage and training time. On contrast, our cross-view module can easily handle the different numbers of viewpoints presented in different datasets. In terms of condition adherence, UniMLVG achieve the SOTA results, improving $mIoU_{road}$ and $mIoU_{vehicle}$ by 8.8% and 7.8%, respectively, over the second-best method. For mAP, we outperform all other methods except DiVE [23]. In contrast to DiVE, UniMLVG does not assign distinct classifier-free guidance scales for each condition, significantly reducing inference time. Furthermore, rather than using the parameter-heavy ControlNet [61], UniMLVG employs a lightweight adapter, enabling more flexible and efficient condition integration.

3Dbox	HDmap	Cam. id.	Cam. ray.	FVD↓	FID↓
				242.46	34.55
✓				79.30	12.80
	✓			79.18	11.86
✓	✓			82.13	11.91
✓	✓	✓		82.76	11.74
✓	✓		✓	76.52	11.71

Table 2. **Ablation studies on 3D conditions and camera pose modeling.** Cam. id. and Cam. ray. represent implicit and explicit modeling, respectively.

Controllability. Our model supports 3D condition control as well as text-based control capabilities. In Figure 1(c), we generate realistic scenes using 3D conditions obtained from the simulation engine CALAR [9]. Notably, different from style transfer methods, our generation is not strictly constrained to transforming the content of simulated scenes. Instead, our model takes the general 3D information such as 3D bounding boxes and HDMaps as inputs and leverages real-world knowledge to generate plausible scenes that align with the distribution of the training data. Specifically, elements such as roads, mountains, and trees are generated with appearances that more accurately reflect how they would look in the real world. This task is highly meaningful because, in simulation, we can create various corner cases, and the model can reimagine these scenarios as real-world conditions, thereby addressing the scarcity of such data. For textual control, the model illustrates strong zero-shot generalizability and impressive editing capabilities under extreme transformations. As shown in Figures 1(d) and 4, even though the nuScenes dataset does not contain any snowy, our model can still edit the weather of nuScene multi-view videos in both daytime and nighttime. Additionally, the generated videos accurately present real-world details such as snow accumulating on the roadside, bare trees during winter, and reflective road surfaces due to rain.

Diversity & Consistency. One primary consideration of driving video generation models is the diversity of the results, as this task is fundamentally intended to address the scarcity of annotated data. In Figure 5, we provide examples to showcase the diversity of our model’s output. The surroundings such as weather, buildings and cars varies from cases to cases, while the generated results strictly follow the real conditions in terms of road layout and vehicle positions. Providing multi-view consistent videos helps enhance the perception capabilities of autonomous driving



Figure 5. **Examples of scene generation diversity under various weather conditions.** (a) Under sunny conditions, the appearance and number of houses, cloud positions, and sunlight direction differ from the ground truth (GT). (b) Under cloudy conditions, the appearance of houses and the colors of nearby vehicles differ from GT. (c) Under rainy conditions, both the appearance of houses and vehicles deviate from GT. The top row displays the ground truth.



Figure 6. **Examples of scene generation consistency.** The lane markings and bushes at the junction of viewpoints remain consistent both during the day and at night.

algorithms. In Figure 6, we present examples of multi-view consistency under both daytime and nighttime conditions. We can observe that lane markings and vegetation remain seamlessly continuous at the boundaries between viewpoints. Please refer to the supplementary materials for more diverse and consistent examples.

4.3. Ablation Studies

We conduct a series of ablation studies to evaluate the distinct contributions of multi-condition, multi-task, multi-dataset and multi-stage training. All the following evaluation metrics are reported on the nuScenes validation set.

Multi-condition. We compare the experimental results for

N	O	W&A	FVD↓	FID↓
✓			82.26	11.83
✓	✓		76.52	11.71
✓	✓	✓	68.80	10.97

Table 3. **Ablations of Multi-dataset.** N, O, W, A represent nuScenes, OpenDV-Youtube, Waymo and Argoverse2, respectively.

Stage	FVD↓	FID↓
Stage I	149.70	30.50
Stage II	64.44	8.82
Stage III	60.11	8.75

Table 4. **Ablations Studies of Multi-stage.** Our multi-stage training strategy can significantly improve the generation quality and consistency.

different combinations of the four conditions, as shown in Table 2. We find that incorporating 3D conditions lead to substantial improvement in FVD and FID, as the 3D information helps the model interpret the driving scene. In addition, we also conduct the comparison between implicit (Cam.id.) and explicit (Cam.ray.) camera pose modeling. Compared to Cam.ray., Cam.id. used in [12] encodes the camera’s intrinsic and extrinsic parameters into a vector, which is handled as global information like textual inputs. The results show that the explicit modeling approach not only improves video continuity by 6.8% but also slightly enhances image quality. This suggests that explicitly incorporating positional relationships between viewpoints into the

VP(%)	IP(%)	FVD↓	FID↓	VP(%)	VG(%)	FVD↓	FID↓	VP(%)	IG(%)	FVD↓	FID↓
100	0	76.52	11.71	100	0	76.52	11.71	100	0	76.52	11.71
95	5	69.46	11.03	95	5	71.30	11.54	95	5	63.36	11.21
90	10	72.71	11.91	90	10	64.88	11.66	90	10	59.44	10.90
80	20	74.74	11.93	80	20	77.50	12.16	80	20	66.17	10.89
70	30	64.05	11.45	70	30	89.14	12.55	60	40	79.68	11.74
60	40	70.26	11.52	60	40	81.08	11.60	40	60	76.06	11.57

(a) Different ratios of VP and IP.

(b) Different ratios of VP and VG.

(c) Different ratios of VP and IG.

Table 5. Ablation Studies of Multi-task.



Figure 7. **Comparison of long-term video generation between VP, VP+IP, and VP+VG.** Introducing IP and VG tasks on top of VP can enhance the quality of frames after multiple autoregressive iterations.

model enhances its understanding of driving scenes. Additionally, the implicit modeling approach does not improve the model’s performance.

Multi-dataset. Table 3 shows the results of training on the nuScenes [5] dataset with and without pretraining weights from a single-view dataset. The results clearly demonstrate that leveraging a large amount of single-view data significantly enhances the continuity and quality of the videos. This indicates that substantial unlabeled single-view street scene sequential data can effectively enhance the model’s ability to imagine and predict future scenes. Additionally, by integrating two multi-view video datasets, Waymo and Argoverse2, for joint training, we achieved a 6.7% improvement in FVD. This demonstrates the model’s scalability and highlights the critical role of diverse data in enhancing its understanding of driving scenes.

Multi-task. Tab. 5 shows the ablation study results across multiple tasks. We used VP as our primary generation task and then combined it sequentially with other tasks to determine an optimal multi-task ratio. In general, the appropriate combination of each task improves the quality of generation. Tab. 5 (a) and Tab. 5 (b) show that IP and VG primarily enhance video consistency, both applying masks on the reference frames and encourage the model to focus on using adjacent frames to ensure temporally consistent rather than relying excessively on the reference frame. Notably, intro-

ducing these two tasks greatly improves the quality of long video generation, as shown in Figure 7. Moreover, Table 5 (c) indicates that the IG task improves both video consistency and quality. By randomly dropping the temporal module, UniMLVG learn to assign different functions to different models. The temporal module focuses more on maintaining temporal consistency, while the cross-view module is dedicated to generating multi-view consistent frames.

Multi-stage. We employ a multi-stage training strategy to ensure that the model can be trained both efficiently and stably. The performance at different stages is shown in Table 4. We find that training on large-scale single-view datasets allows the model to develop generalization and some kind of temporal generation capability. Without having seen any nuScenes data, the model achieves an FVD of 149.70 on the nuScenes validation set, already surpassing MagicDrive [12]. This indicates that the model has already developed the generalization ability to predict future frames based on reference frames. In the second stage, the model achieves a substantial leap in both temporal consistency and image quality. In this phase, the model not only relies on temporal information and cross-view integration but also possesses condition controllability. Finally, we performed full fine-tuning on the model to unlock its potential, resulting in further improvements in the metrics.

5. Conclusion

To address the growing demand for generating realistic surround-view videos in autonomous driving, we propose a unified multi-view long video generation framework that supports multi-dataset training and offers versatile condition control capabilities. Specifically, we introduce a multi-task, multi-stage training strategy that effectively alleviates scene inconsistencies during long-term video generation. Moreover, by incorporating diverse datasets, image-level descriptions, and 3D conditions, our model achieves flexible control, such as generating snowy nuScenes scenes that do not exist in the original dataset. Furthermore, we are the first to introduce explicit camera viewpoint modeling for this task, which significantly enhances the consistency of video generation. We hope that our work can contribute to advancing the development of autonomous driving.

References

- [1] Latte: Latent diffusion transformer for video generation. *arXiv preprint arXiv:2401.03048*, 2024. 2
- [2] Multimodal perception and comprehension of corner cases in autonomous driving. URL: <https://coda-dataset.github.io/w-coda2024/track2/>, 2024. 5
- [3] Andreas Blattmann, Tim Dockhorn, Sumith Kulal, Daniel Mendelevitch, Maciej Kilian, Dominik Lorenz, Yam Levi, Zion English, Vikram Voleti, Adam Letts, et al. Stable video diffusion: Scaling latent video diffusion models to large datasets. *arXiv preprint arXiv:2311.15127*, 2023. 3
- [4] Tim Brooks, Bill Peebles, Connor Holmes, Will DePue, Yufei Guo, Li Jing, David Schnurr, Joe Taylor, Troy Luhman, Eric Luhman, Clarence Ng, Ricky Wang, and Aditya Ramesh. Video generation models as world simulators. 2024. 2
- [5] Holger Caesar, Varun Bankiti, Alex H Lang, Sourabh Vora, Venice Erin Liong, Qiang Xu, Anush Krishnan, Yu Pan, Giancarlo Baldan, and Oscar Beijbom. nuscenes: A multimodal dataset for autonomous driving. In *Proceedings of the IEEE/CVF conference on computer vision and pattern recognition*, pages 11621–11631, 2020. 5, 8
- [6] Mehdi Cherti, Romain Beaumont, Ross Wightman, Mitchell Wortsman, Gabriel Ilharco, Cade Gordon, Christoph Schuhmann, Ludwig Schmidt, and Jenia Jitsev. Reproducible scaling laws for contrastive language-image learning. In *Proceedings of the IEEE/CVF Conference on Computer Vision and Pattern Recognition*, pages 2818–2829, 2023. 4
- [7] Aidan Clark, Jeff Donahue, and Karen Simonyan. Adversarial video generation on complex datasets. *arXiv preprint arXiv:1907.06571*, 2019. 2
- [8] Emily Denton and Rob Fergus. Stochastic video generation with a learned prior. In *International conference on machine learning*, pages 1174–1183. PMLR, 2018. 2
- [9] Alexey Dosovitskiy, German Ros, Felipe Codevilla, Antonio Lopez, and Vladlen Koltun. Carla: An open urban driving simulator. In *Conference on robot learning*, pages 1–16. PMLR, 2017. 6
- [10] Patrick Esser, Sumith Kulal, Andreas Blattmann, Rahim Entezari, Jonas Müller, Harry Saini, Yam Levi, Dominik Lorenz, Axel Sauer, Frederic Boesel, et al. Scaling rectified flow transformers for high-resolution image synthesis. In *Forty-first International Conference on Machine Learning*, 2024. 2, 3, 4, 5, 1
- [11] Flux. Flux ai studio. URL: <https://fluxai.studio/>, 2024. 3
- [12] Ruiyuan Gao, Kai Chen, Enze Xie, Lanqing Hong, Zhenguo Li, Dit-Yan Yeung, and Qiang Xu. Magicdrive: Street view generation with diverse 3d geometry control. *arXiv preprint arXiv:2310.02601*, 2023. 2, 3, 5, 7, 8, 1
- [13] Ruiqi Gao, Aleksander Holynski, Philipp Henzler, Arthur Brussee, Ricardo Martin-Brualla, Pratul Srinivasan, Jonathan T Barron, and Ben Poole. Cat3d: Create anything in 3d with multi-view diffusion models. *arXiv preprint arXiv:2405.10314*, 2024. 4
- [14] Shenyan Gao, Jiazhi Yang, Li Chen, Kashyap Chitta, Yihang Qiu, Andreas Geiger, Jun Zhang, and Hongyang Li. Vista: A generalizable driving world model with high fidelity and versatile controllability. *arXiv preprint arXiv:2405.17398*, 2024. 2
- [15] Yuwei Guo, Ceyuan Yang, Anyi Rao, Zhengyang Liang, Yaohui Wang, Yu Qiao, Maneesh Agrawala, Dahua Lin, and Bo Dai. Animatediff: Animate your personalized text-to-image diffusion models without specific tuning. *arXiv preprint arXiv:2307.04725*, 2023. 2
- [16] Jiawei He, Andreas Lehrmann, Joseph Marino, Greg Mori, and Leonid Sigal. Probabilistic video generation using holistic attribute control. In *Proceedings of the European Conference on Computer Vision (ECCV)*, pages 452–467, 2018. 2
- [17] Martin Heusel, Hubert Ramsauer, Thomas Unterthiner, Bernhard Nessler, and Sepp Hochreiter. Gans trained by a two time-scale update rule converge to a local nash equilibrium. *Advances in neural information processing systems*, 30, 2017. 5
- [18] Jonathan Ho, Tim Salimans, Alexey Gritsenko, William Chan, Mohammad Norouzi, and David J Fleet. Video diffusion models. *Advances in Neural Information Processing Systems*, 35:8633–8646, 2022. 2, 6
- [19] Jun-Ting Hsieh, Bingbin Liu, De-An Huang, Li F Fei-Fei, and Juan Carlos Niebles. Learning to decompose and disentangle representations for video prediction. *Advances in neural information processing systems*, 31, 2018. 2
- [20] Anthony Hu, Lloyd Russell, Hudson Yeo, Zak Murez, George Fedoseev, Alex Kendall, Jamie Shotton, and Gianluca Corrado. Gaia-1: A generative world model for autonomous driving. *arXiv preprint arXiv:2309.17080*, 2023. 2
- [21] Yihan Hu, Jiazhi Yang, Li Chen, Keyu Li, Chonghao Sima, Xizhou Zhu, Siqi Chai, Senyao Du, Tianwei Lin, Wenhai Wang, et al. Planning-oriented autonomous driving. In *Proceedings of the IEEE/CVF Conference on Computer Vision and Pattern Recognition*, pages 17853–17862, 2023. 2
- [22] Bo Jiang, Shaoyu Chen, Qing Xu, Bencheng Liao, Jiajie Chen, Helong Zhou, Qian Zhang, Wenyu Liu, Chang Huang, and Xinggang Wang. Vad: Vectorized scene representation for efficient autonomous driving. In *Proceedings of the IEEE/CVF International Conference on Computer Vision*, pages 8340–8350, 2023. 2
- [23] Junpeng Jiang, Gangyi Hong, Lijun Zhou, Enhui Ma, Hengtong Hu, Xia Zhou, Jie Xiang, Fan Liu, Kaicheng Yu, Haiyang Sun, et al. Dive: Dit-based video generation with enhanced control. *arXiv preprint arXiv:2409.01595*, 2024. 2, 3, 5, 6, 1
- [24] Seung Wook Kim, Jonah Philion, Antonio Torralba, and Sanja Fidler. Drivegan: Towards a controllable high-quality neural simulation. In *Proceedings of the IEEE/CVF Conference on Computer Vision and Pattern Recognition*, pages 5820–5829, 2021. 2, 5
- [25] Yitong Li, Zhe Gan, Yelong Shen, Jingjing Liu, Yu Cheng, Yuxin Wu, Lawrence Carin, David Carlson, and Jianfeng Gao. Storygan: A sequential conditional gan for story visualization. In *Proceedings of the IEEE/CVF conference on computer vision and pattern recognition*, pages 6329–6338, 2019. 2

- [26] Yaron Lipman, Ricky TQ Chen, Heli Ben-Hamu, Maximilian Nickel, and Matt Le. Flow matching for generative modeling. *arXiv preprint arXiv:2210.02747*, 2022. 3
- [27] Xingchao Liu, Chengyue Gong, and Qiang Liu. Flow straight and fast: Learning to generate and transfer data with rectified flow. *arXiv preprint arXiv:2209.03003*, 2022. 3
- [28] Zhijian Liu, Haotian Tang, Alexander Amini, Xinyu Yang, Huizi Mao, Daniela L Rus, and Song Han. Bevfusion: Multi-task multi-sensor fusion with unified bird’s-eye view representation. In *2023 IEEE international conference on robotics and automation (ICRA)*, pages 2774–2781. IEEE, 2023. 5
- [29] Ilya Loshchilov, Frank Hutter, et al. Fixing weight decay regularization in adam. *arXiv preprint arXiv:1711.05101*, 5, 2017. 5
- [30] Jianbiao Mei, Yukai Ma, Xuemeng Yang, Licheng Wen, Tiantian Wei, Min Dou, Botian Shi, and Yong Liu. Dreamforge: Motion-aware autoregressive video generation for multi-view driving scenes. *arXiv preprint arXiv:2409.04003*, 2024. 2, 3, 5
- [31] Chong Mou, Xintao Wang, Liangbin Xie, Yanze Wu, Jian Zhang, Zhongang Qi, and Ying Shan. T2i-adapter: Learning adapters to dig out more controllable ability for text-to-image diffusion models. In *Proceedings of the AAAI Conference on Artificial Intelligence*, pages 4296–4304, 2024. 4
- [32] Open-Sora. Open-sora. URL: <https://github.com/hpcaitech/Open-Sora>, 2024. 2, 3
- [33] Ethan Perez, Florian Strub, Harm De Vries, Vincent Dumoulin, and Aaron Courville. Film: Visual reasoning with a general conditioning layer. In *Proceedings of the AAAI conference on artificial intelligence*, 2018. 4
- [34] Chenyang Qi, Xiaodong Cun, Yong Zhang, Chenyang Lei, Xintao Wang, Ying Shan, and Qifeng Chen. Fatezero: Fusing attentions for zero-shot text-based video editing. In *Proceedings of the IEEE/CVF International Conference on Computer Vision*, pages 15932–15942, 2023. 2
- [35] Alec Radford, Jeffrey Wu, Rewon Child, David Luan, Dario Amodei, Ilya Sutskever, et al. Language models are unsupervised multitask learners. *OpenAI blog*, 1(8):9, 2019. 1
- [36] Alec Radford, Jong Wook Kim, Chris Hallacy, Aditya Ramesh, Gabriel Goh, Sandhini Agarwal, Girish Sastry, Amanda Askell, Pamela Mishkin, Jack Clark, et al. Learning transferable visual models from natural language supervision. In *International conference on machine learning*, pages 8748–8763. PMLR, 2021. 4
- [37] Colin Raffel, Noam Shazeer, Adam Roberts, Katherine Lee, Sharan Narang, Michael Matena, Yanqi Zhou, Wei Li, and Peter J Liu. Exploring the limits of transfer learning with a unified text-to-text transformer. *Journal of machine learning research*, 21(140):1–67, 2020. 4
- [38] Robin Rombach, Andreas Blattmann, Dominik Lorenz, Patrick Esser, and Björn Ommer. High-resolution image synthesis with latent diffusion models. In *Proceedings of the IEEE/CVF conference on computer vision and pattern recognition*, pages 10684–10695, 2022. 3
- [39] Masaki Saito, Shunta Saito, Masanori Koyama, and Sosuke Kobayashi. Train sparsely, generate densely: Memory-efficient unsupervised training of high-resolution temporal gan. *International Journal of Computer Vision*, 128(10): 2586–2606, 2020. 2
- [40] Mehdi SM Sajjadi, Henning Meyer, Etienne Pot, Urs Bergmann, Klaus Greff, Noha Radwan, Suhani Vora, Mario Lučić, Daniel Duckworth, Alexey Dosovitskiy, et al. Scene representation transformer: Geometry-free novel view synthesis through set-latent scene representations. In *Proceedings of the IEEE/CVF Conference on Computer Vision and Pattern Recognition*, pages 6229–6238, 2022. 4
- [41] Younggyo Seo, Kimin Lee, Fangchen Liu, Stephen James, and Pieter Abbeel. Harp: Autoregressive latent video prediction with high-fidelity image generator. In *2022 IEEE International Conference on Image Processing (ICIP)*, pages 3943–3947. IEEE, 2022. 2
- [42] Ivan Skorokhodov, Sergey Tulyakov, and Mohamed Elhoseiny. Stylegan-v: A continuous video generator with the price, image quality and perks of stylegan2. In *Proceedings of the IEEE/CVF conference on computer vision and pattern recognition*, pages 3626–3636, 2022. 2
- [43] Pei Sun, Henrik Kretzschmar, Xerxes Dotiwalla, Aurelien Chouard, Vijaysai Patnaik, Paul Tsui, James Guo, Yin Zhou, Yuning Chai, Benjamin Caine, et al. Scalability in perception for autonomous driving: Waymo open dataset. In *Proceedings of the IEEE/CVF conference on computer vision and pattern recognition*, pages 2446–2454, 2020. 5
- [44] Zineng Tang, Ziyi Yang, Chenguang Zhu, Michael Zeng, and Mohit Bansal. Any-to-any generation via composable diffusion. *Advances in Neural Information Processing Systems*, 36, 2024. 2
- [45] Thomas Unterthiner, Sjoerd Van Steenkiste, Karol Kurach, Raphael Marinier, Marcin Michalski, and Sylvain Gelly. Towards accurate generative models of video: A new metric & challenges. *arXiv preprint arXiv:1812.01717*, 2018. 5
- [46] A Vaswani. Attention is all you need. *Advances in Neural Information Processing Systems*, 2017. 4
- [47] Ting-Chun Wang, Ming-Yu Liu, Jun-Yan Zhu, Guilin Liu, Andrew Tao, Jan Kautz, and Bryan Catanzaro. Video-to-video synthesis. *arXiv preprint arXiv:1808.06601*, 2018. 2
- [48] Wenhai Wang, Jiangwei Xie, ChuanYang Hu, Haoming Zou, Jianan Fan, Wenwen Tong, Yang Wen, Silei Wu, Hanming Deng, Zhiqi Li, et al. Drivemlm: Aligning multi-modal large language models with behavioral planning states for autonomous driving. *arXiv preprint arXiv:2312.09245*, 2023. 5, 1
- [49] Xiaofeng Wang, Zheng Zhu, Guan Huang, Xinze Chen, Jiagang Zhu, and Jiwen Lu. Drivedreamer: Towards real-world-driven world models for autonomous driving. *arXiv preprint arXiv:2309.09777*, 2023. 2, 3, 5
- [50] Yuqi Wang, Jiawei He, Lue Fan, Hongxin Li, Yuntao Chen, and Zhaoxiang Zhang. Driving into the future: Multiview visual forecasting and planning with world model for autonomous driving. In *Proceedings of the IEEE/CVF Conference on Computer Vision and Pattern Recognition*, pages 14749–14759, 2024. 2, 3, 5, 1
- [51] Zhouxia Wang, Ziyang Yuan, Xintao Wang, Yaowei Li, Tianshui Chen, Menghan Xia, Ping Luo, and Ying Shan. Motionctrl: A unified and flexible motion controller for

- video generation. In *ACM SIGGRAPH 2024 Conference Papers*, pages 1–11, 2024. 2
- [52] Benjamin Wilson, William Qi, Tanmay Agarwal, John Lambert, Jagjeet Singh, Siddhesh Khandelwal, Bowen Pan, Ratnesh Kumar, Andrew Hartnett, Jhony Kaesemodel Pontes, et al. Argoverse 2: Next generation datasets for self-driving perception and forecasting. *arXiv preprint arXiv:2301.00493*, 2023. 5
- [53] Chenfei Wu, Lun Huang, Qianxi Zhang, Binyang Li, Lei Ji, Fan Yang, Guillermo Sapiro, and Nan Duan. Godiva: Generating open-domain videos from natural descriptions. *arXiv preprint arXiv:2104.14806*, 2021. 2
- [54] Chenfei Wu, Jian Liang, Lei Ji, Fan Yang, Yuejian Fang, Daxin Jiang, and Nan Duan. Nüwa: Visual synthesis pre-training for neural visual world creation. In *European conference on computer vision*, pages 720–736. Springer, 2022. 2
- [55] Jay Zhangjie Wu, Yixiao Ge, Xintao Wang, Stan Weixian Lei, Yuchao Gu, Yufei Shi, Wynne Hsu, Ying Shan, Xiaoju Qie, and Mike Zheng Shou. Tune-a-video: One-shot tuning of image diffusion models for text-to-video generation. In *Proceedings of the IEEE/CVF International Conference on Computer Vision*, pages 7623–7633, 2023. 2
- [56] Wilson Yan, Yunzhi Zhang, Pieter Abbeel, and Aravind Srinivas. Videogpt: Video generation using vq-vae and transformers. *arXiv preprint arXiv:2104.10157*, 2021. 2
- [57] Jiazhi Yang, Shenyuan Gao, Yihang Qiu, Li Chen, Tianyu Li, Bo Dai, Kashyap Chitta, Penghao Wu, Jia Zeng, Ping Luo, et al. Generalized predictive model for autonomous driving. In *Proceedings of the IEEE/CVF Conference on Computer Vision and Pattern Recognition*, pages 14662–14672, 2024. 2, 5
- [58] Zhenpei Yang, Yuning Chai, Dragomir Anguelov, Yin Zhou, Pei Sun, Dumitru Erhan, Sean Rafferty, and Henrik Kretschmar. Surfelgan: Synthesizing realistic sensor data for autonomous driving. In *Proceedings of the IEEE/CVF Conference on Computer Vision and Pattern Recognition*, pages 11118–11127, 2020. 2
- [59] Hangjie Yuan, Shiwei Zhang, Xiang Wang, Yujie Wei, Tao Feng, Yining Pan, Yingya Zhang, Ziwei Liu, Samuel Albanie, and Dong Ni. Instructvideo: instructing video diffusion models with human feedback. In *Proceedings of the IEEE/CVF Conference on Computer Vision and Pattern Recognition*, pages 6463–6474, 2024. 2
- [60] Ekim Yurtsever, Jacob Lambert, Alexander Carballo, and Kazuya Takeda. A survey of autonomous driving: Common practices and emerging technologies. *IEEE access*, 8:58443–58469, 2020. 2
- [61] Lvmin Zhang, Anyi Rao, and Maneesh Agrawala. Adding conditional control to text-to-image diffusion models. In *Proceedings of the IEEE/CVF International Conference on Computer Vision*, pages 3836–3847, 2023. 3, 6
- [62] Guosheng Zhao, Xiaofeng Wang, Zheng Zhu, Xinze Chen, Guan Huang, Xiaoyi Bao, and Xingang Wang. Drivedreamer-2: Llm-enhanced world models for diverse driving video generation. *arXiv preprint arXiv:2403.06845*, 2024. 2, 3, 4, 5, 6, 1
- [63] Xuanlei Zhao, Xiaolong Jin, Kai Wang, and Yang You. Real-time video generation with pyramid attention broadcast. *arXiv preprint arXiv:2408.12588*, 2024. 2
- [64] Brady Zhou and Philipp Krähenbühl. Cross-view transformers for real-time map-view semantic segmentation. In *Proceedings of the IEEE/CVF conference on computer vision and pattern recognition*, pages 13760–13769, 2022. 5
- [65] Shenhao Zhu, Junming Leo Chen, Zuozhuo Dai, Qingkun Su, Yinghui Xu, Xun Cao, Yao Yao, Hao Zhu, and Siyu Zhu. Champ: Controllable and consistent human image animation with 3d parametric guidance. *arXiv preprint arXiv:2403.14781*, 2024. 2

UniMLVG: Unified Framework for Multi-view Long Video Generation with Comprehensive Control Capabilities for Autonomous Driving

Supplementary Material

6. Details on Explicit Perspective Modeling

Explicit perspective modeling aims to inject spatial information into UniMLVG to enhance the coherence of generated videos. Specifically, we utilize a set of the camera’s intrinsic parameters $K \in \mathbb{R}^{B \times T \times V \times 3 \times 3}$ and the extrinsic transformations $E \in \mathbb{R}^{B \times T \times V \times 3 \times 4}$, which map viewpoints to the forward-facing perspective of the first reference frame. In this way, we can directly obtain the camera’s origin coordinates $Ray_o = E_4$, where $E_4 \in \mathbb{R}^{B \times T \times V \times 3}$ represent the latest columns of the last dimensions the camera extrinsic matrices. We extend the camera origins to $\mathbb{R}^{B \times T \times V \times 3 \times H \times W}$ to match the number of video pixels. We then define a three-dimensional pixel plane (in homogeneous coordinates) $P \in \mathbb{R}^{B \times T \times V \times 3 \times H \times W}$ with the same dimensions as the image latent space. Using the scaled camera intrinsic parameters and transformations, the ray directions from the origin to the plane can be computed as follows: $Ray_d = E_{:,3} \times K^{-1} \times P$, $E_{:,3}$ refers to the upper-left 3×3 rotation matrix of the extrinsic matrix E . After transforming the encoded Ray_o and Ray_d through an MLP, the resulting features are added to the image latent before feeding it into the cross-view and temporal modules.

7. Details on fusion of Cross-view and Temporal Information

The fusion of cross-view and temporal information is essential to this task. We believe that the original text-to-image generation model [10] already possesses strong image generation capabilities, requiring only minor modifications to the image latent to achieve cross-view consistency and temporal coherence. Therefore, we simply use a learnable parameter to perform a weighted summation of the outputs from the cross-view or temporal models with the backbone’s image latent. Specifically, both the cross-view and temporal modules are GPT-2-style self-attention mechanisms [35] to make necessary adjustments to the image latent. The fusion process can be formulated as:

$$z_l = \text{Sigmoid}(\alpha) \cdot z'_l + (1 - \text{Sigmoid}(\alpha)) \cdot \mathcal{F}_l(z'_l),$$

where α is a learnable parameter, initially set to 2 to facilitate gradual model training, z'_l denotes the output image latent from the backbone at the l -th layer, and \mathcal{F} represents either the cross-view module or the temporal module. In addition, we found that it is not necessary to add these two modules after every layer of the backbone; adding them at intervals does not affect performance.

8. Details on Image-level Description

In previous works [12, 23, 50, 62], scene descriptions were exclusively used as textual conditions for multi-view video generation. However, such descriptions often lack the fine-grained details necessary for high-quality and consistent generation. To address this limitation, we incorporate image-level descriptions, enabling more precise control over the generation process and improving the consistency and realism of multi-view videos. Specifically, we leverage the multimodal model Drivemlm [48]. For each view, we input the image along with two question prompts: *”Describe the time, weather, environment, objects, and each value should be a single string and less than 20 words.”* and *”Describe objects in this image within about 30 words.”* to generate detailed annotations of the time, weather, environment, and objects present in the viewpoint. Figure 8 presents the statistical information on time, weather, and environment annotations across the four datasets. We can observe that daytime scenes dominate across all four datasets, accounting for more than 80% of the data. In terms of weather, the two most frequently occurring descriptors are *overcast* and *clear sky*. It is worth noting that snowy scenes in Argoverse2 constitute less than 2.6%. However, UniMLVG can still modify weather text conditions to transform scenes under other weather conditions into snowy scenes, demonstrating its robust generalization and semantic understanding capabilities. In terms of environmental descriptions, we can observe the primary focus of data collection for each dataset. For instance, nuScenes, Waymo, and Argoverse2 primarily capture urban street environments, whereas OpenDV-Youtube exhibits a broader range of scenes, including highways and deserts.

9. More Qualitative Results

We provide additional examples to further demonstrate the capabilities of UniMLVG in generating long-duration, multi-view consistent videos. Figures 9, 10 and 11 showcase multi-view long video samples under various weather conditions and times, utilizing reference frames. Conversely, Figures 12, 13 and 14 illustrate multi-view long video samples under similar conditions but without reference frames. Additionally, Figures 15, 16 and 17 demonstrate the transformation of scenes with different times and weather conditions into snowy scenes through text editing. Finally, Figures 18, 19, and 20 showcase the model’s generalization capability, enabling the generation of realistic scenes based on conditions from virtual simulations.

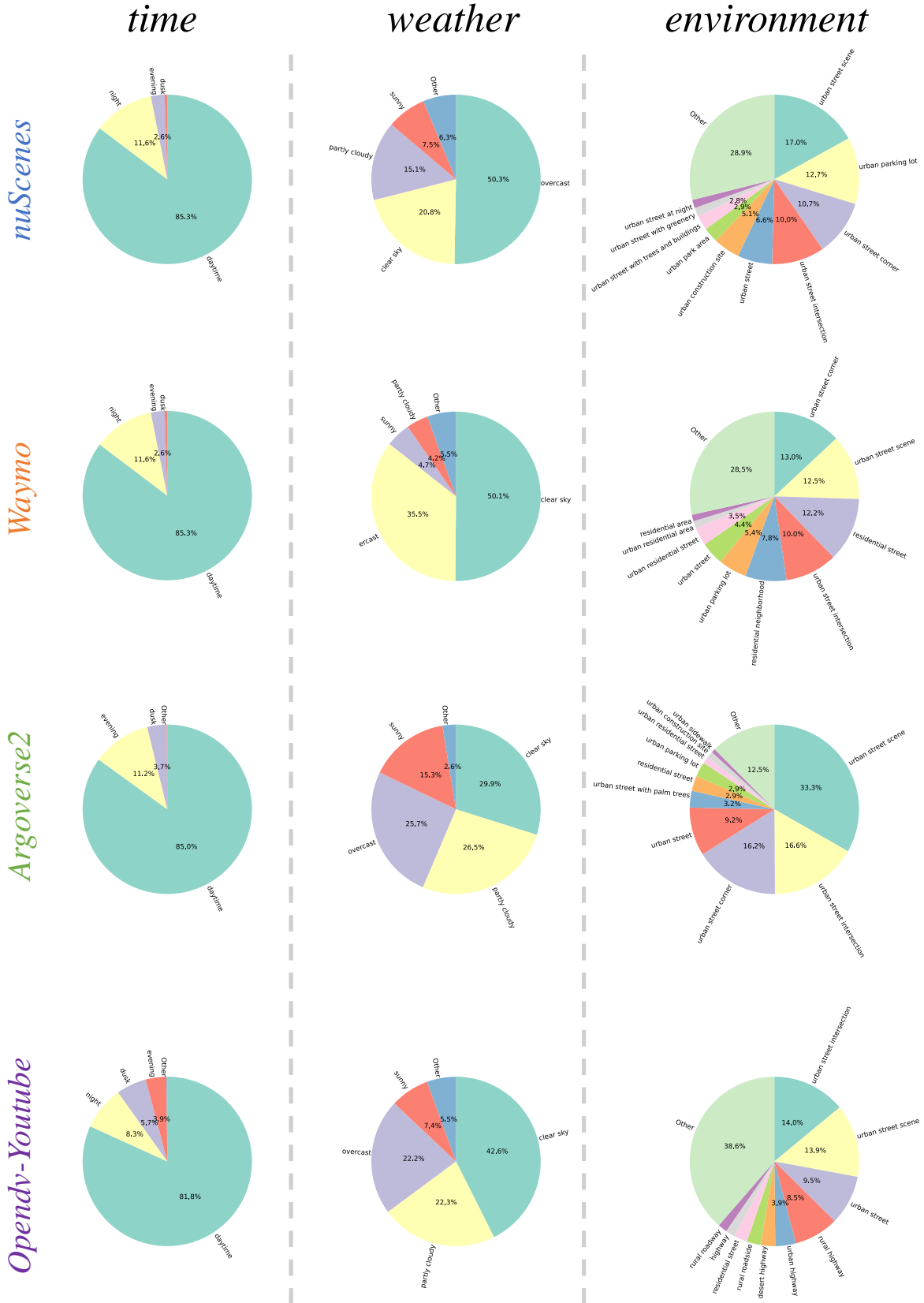


Figure 8. Statistical Analysis of time, weather, and environment in text descriptions on four datasets.

Ground Truth



$t=0s$



$t=2s$



$t=5s$



$t=10s$



$t=15s$



$t=20s$

Generation



$t=0s$



$t=2s$



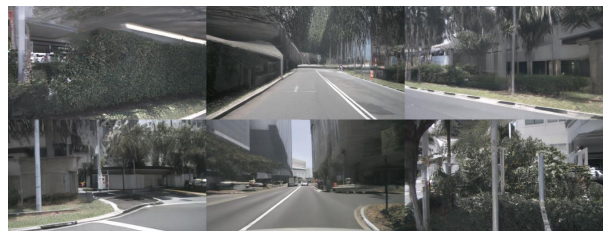
$t=5s$



$t=10s$



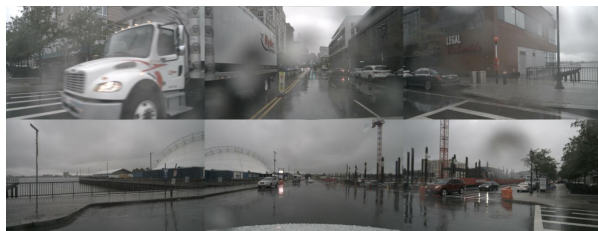
$t=15s$



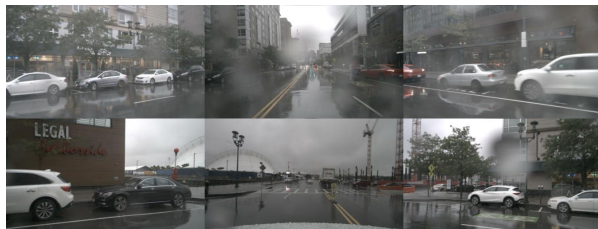
$t=20s$

Figure 9. Sample of 20s multi-view video in a sunny scene with reference frames.

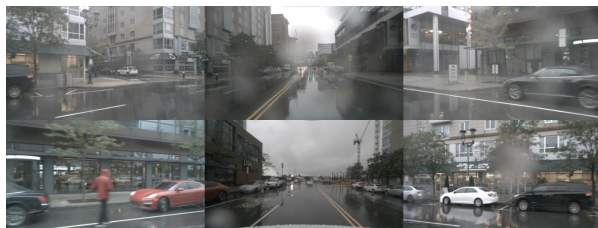
Ground Truth



$t=0s$



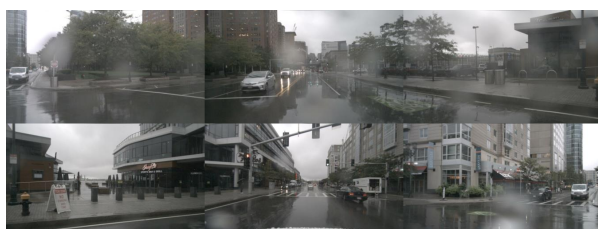
$t=2s$



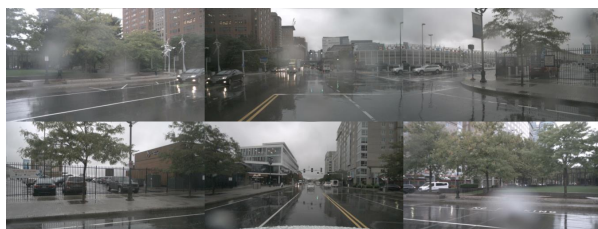
$t=5s$



$t=10s$

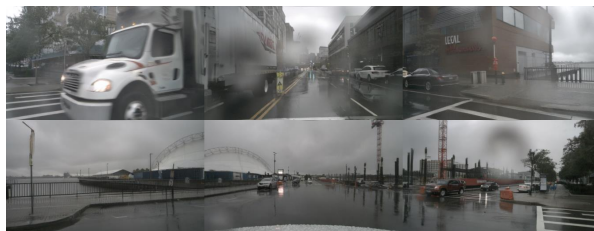


$t=15s$

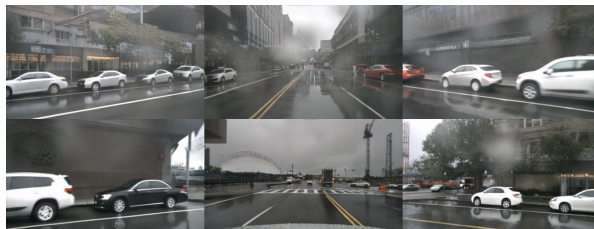


$t=20s$

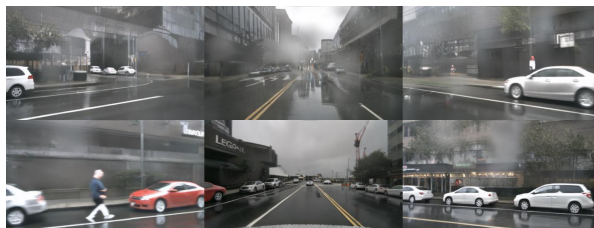
Generation



$t=0s$



$t=2s$



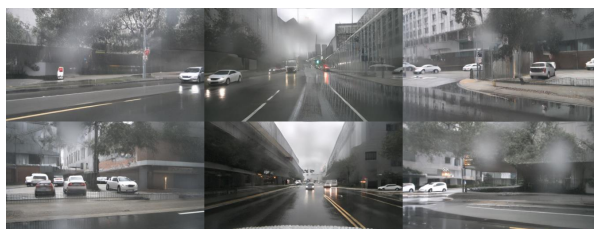
$t=5s$



$t=10s$



$t=15s$



$t=20s$

Figure 10. Sample of 20s multi-view video in a rainy scene with reference frames.

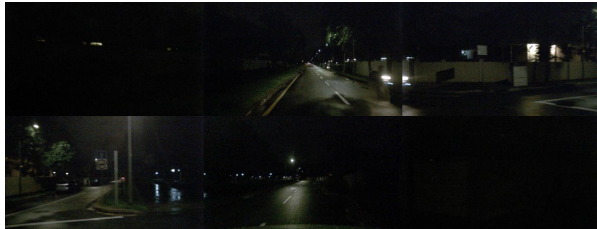
Ground Truth



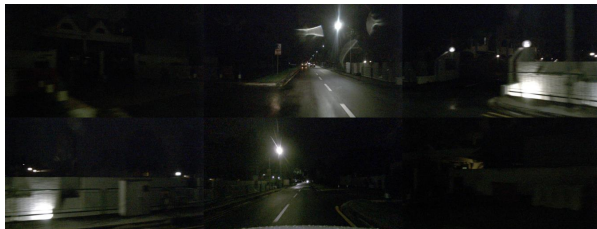
$t=0s$



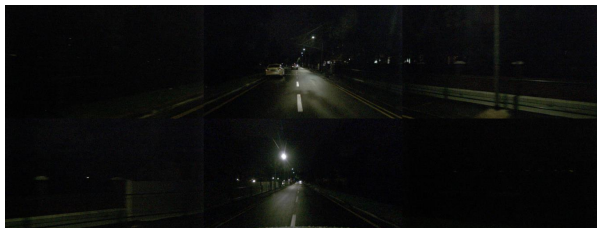
$t=2s$



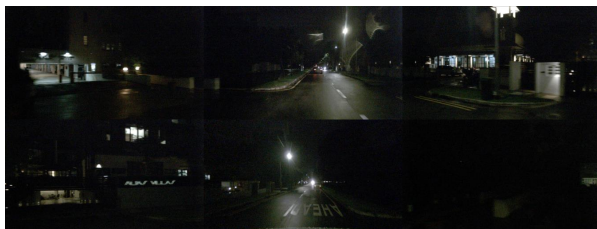
$t=5s$



$t=10s$



$t=15s$



$t=20s$

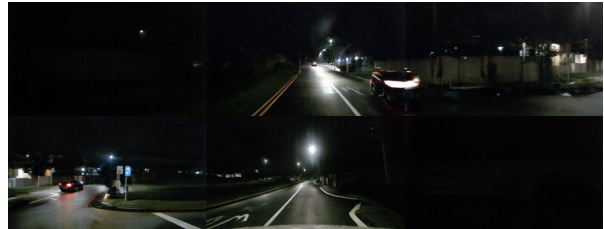
Generation



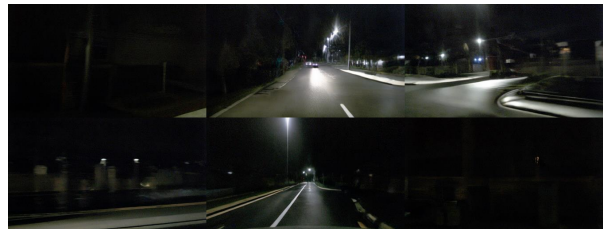
$t=0s$



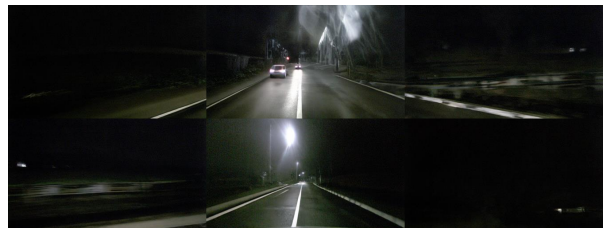
$t=2s$



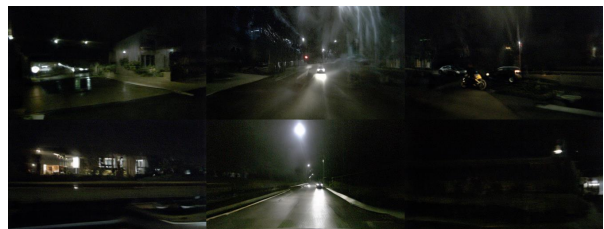
$t=5s$



$t=10s$



$t=15s$



$t=20s$

Figure 11. Sample of 20s multi-view video at night with reference frames.

Ground Truth



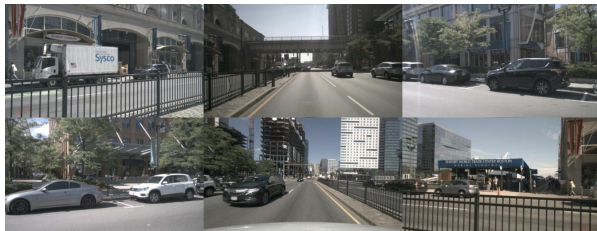
$t=0s$



$t=2s$



$t=5s$



$t=10s$



$t=15s$



$t=20s$

Generation



$t=0s$



$t=2s$



$t=5s$



$t=10s$



$t=15s$



$t=20s$

Figure 12. Sample of 20s multi-view video in a sunny scene without reference frames.

Ground Truth



$t=0s$



$t=2s$



$t=5s$



$t=10s$



$t=15s$



$t=20s$

Generation



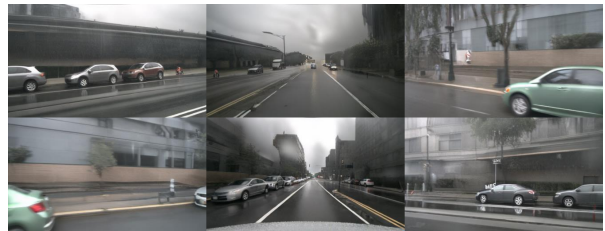
$t=0s$



$t=2s$



$t=5s$



$t=10s$



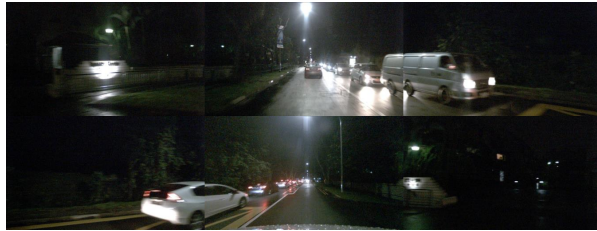
$t=15s$



$t=20s$

Figure 13. Sample of 20s multi-view video in a rainy scene without reference frames.

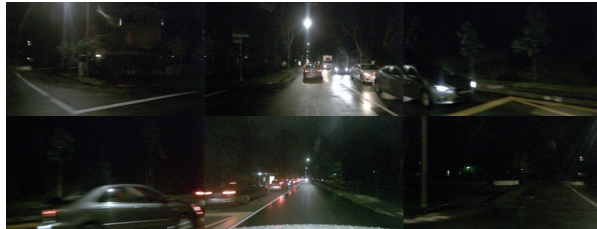
Ground Truth



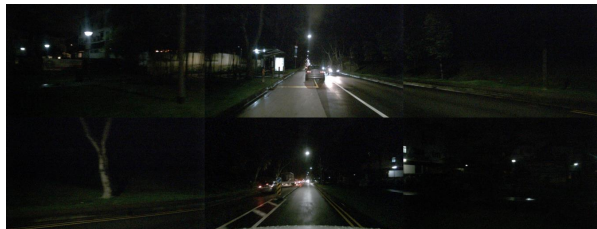
$t=0s$



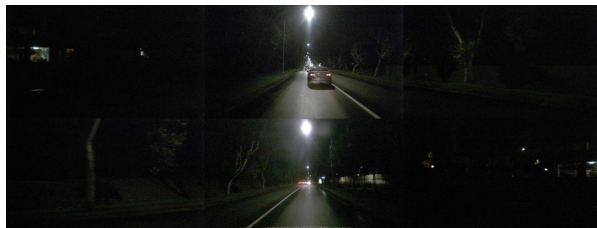
$t=2s$



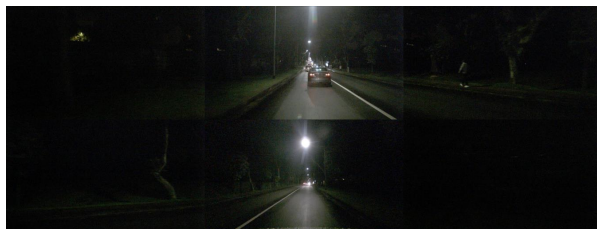
$t=5s$



$t=10s$



$t=15s$



$t=20s$

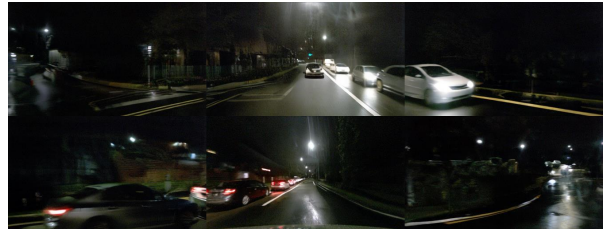
Generation



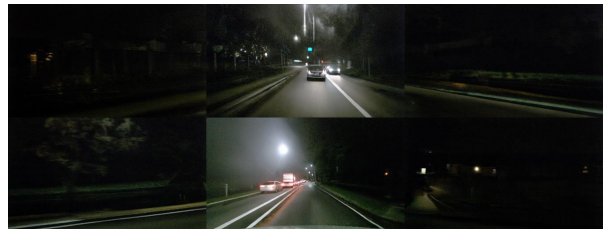
$t=0s$



$t=2s$



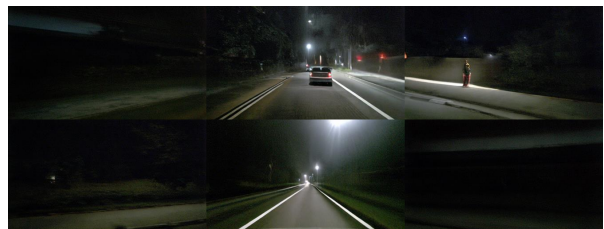
$t=5s$



$t=10s$



$t=15s$



$t=20s$

Figure 14. Sample of 20s multi-view video at night without reference frames..

Ground Truth



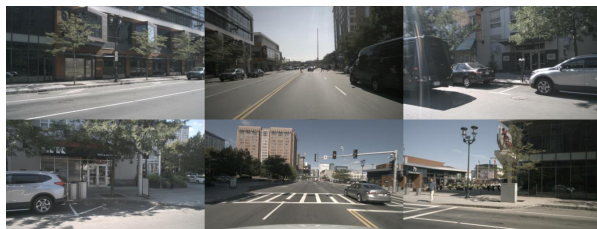
$t=0s$



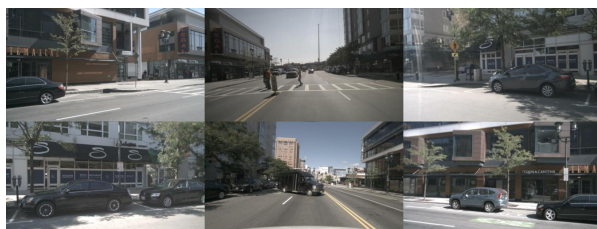
$t=2s$



$t=5s$



$t=10s$

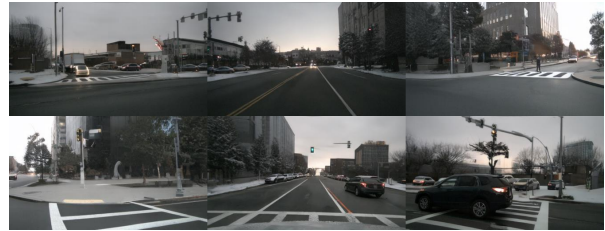


$t=15s$

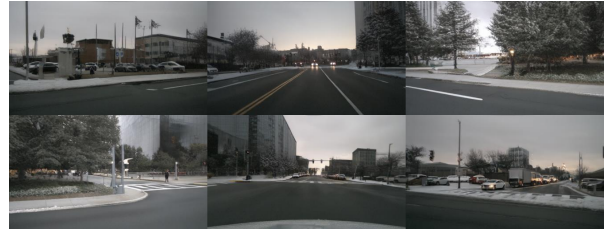


$t=20s$

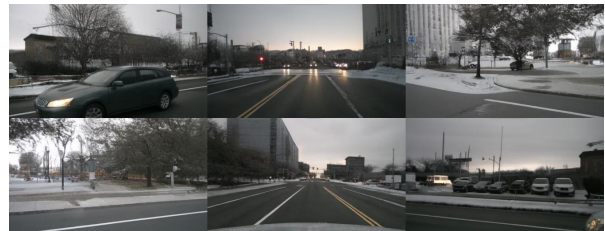
Generation



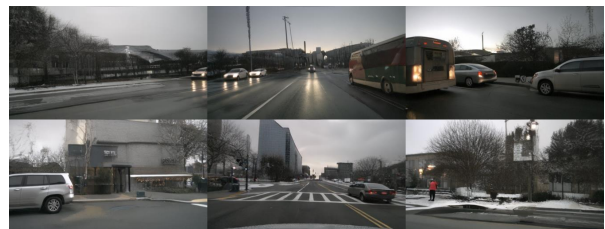
$t=0s$



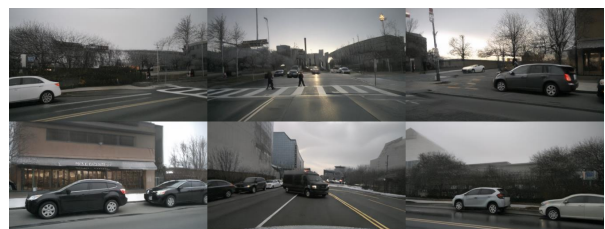
$t=2s$



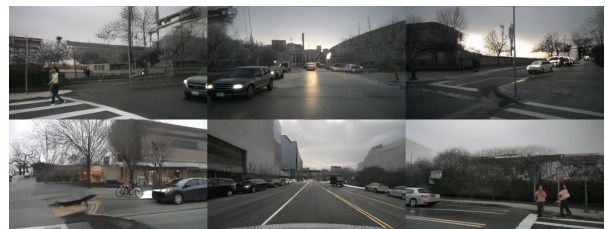
$t=5s$



$t=10s$



$t=15s$



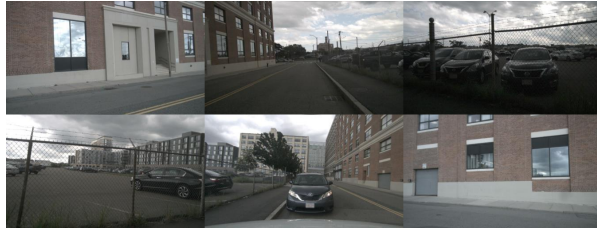
$t=20s$

Figure 15. Sample of a 20s multi-view video transformed from a sunny to a snowy scene through text editing.

Ground Truth



$t=0s$



$t=2s$



$t=5s$



$t=10s$



$t=15s$



$t=20s$

Generation



$t=0s$



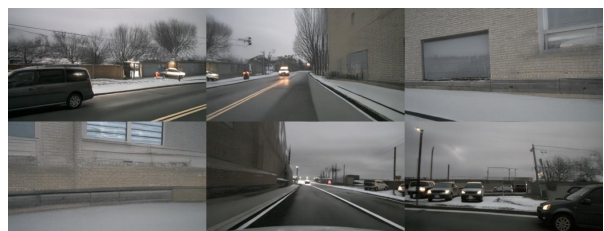
$t=2s$



$t=5s$



$t=10s$



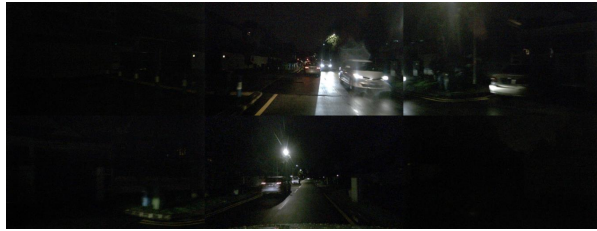
$t=15s$



$t=20s$

Figure 16. Sample of a 20s multi-view video transformed from a cloudy to a snowy scene through text editing.

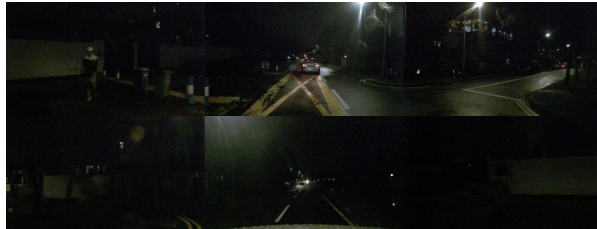
Ground Truth



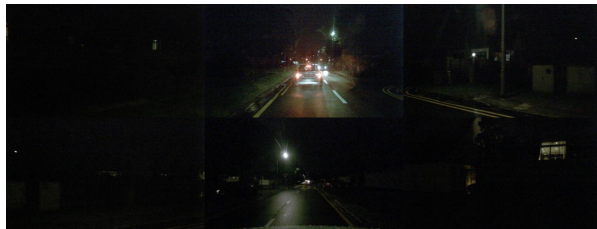
$t=0s$



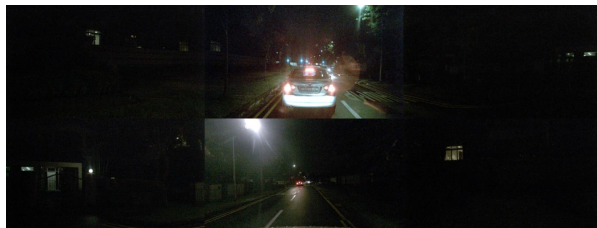
$t=2s$



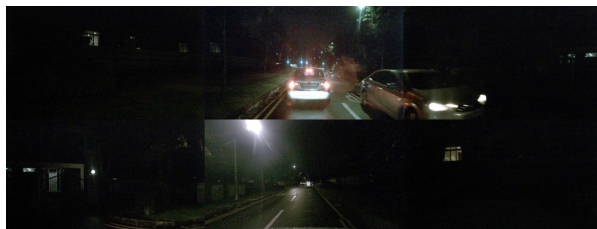
$t=5s$



$t=10s$



$t=15s$



$t=20s$

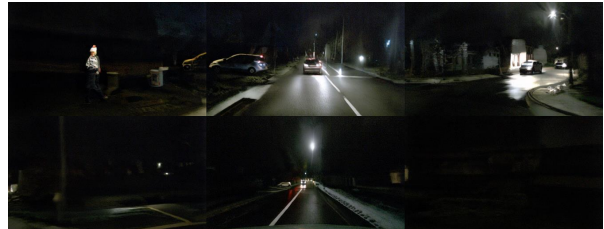
Generation



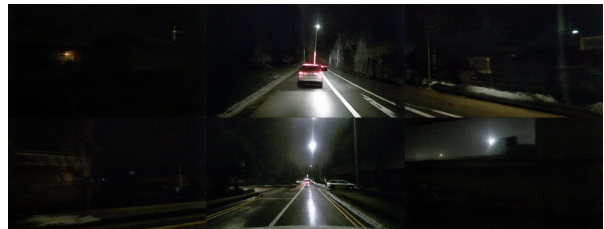
$t=0s$



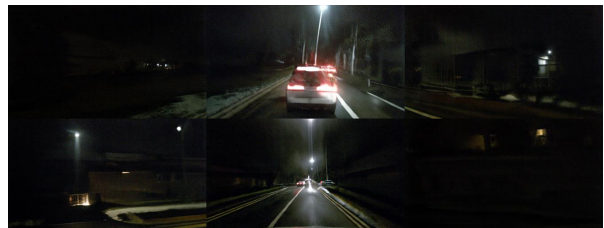
$t=2s$



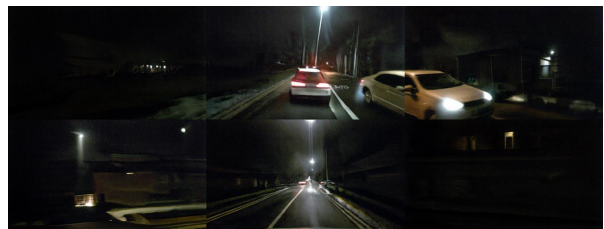
$t=5s$



$t=10s$



$t=15s$



$t=20s$

Figure 17. Sample of a 20s multi-view video generated as a snowy night scene through text editing.

Ground Truth



$t=0s$



$t=2s$



$t=5s$



$t=10s$



$t=15s$



$t=20s$

Generation



$t=0s$



$t=2s$



$t=5s$



$t=10s$



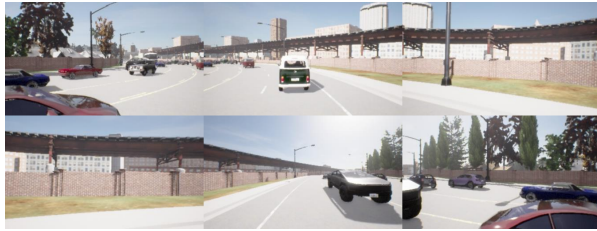
$t=15s$



$t=20s$

Figure 18. Sample of a realistic scene generation based on CARLA conditions.

Ground Truth



$t=0s$



$t=2s$



$t=5s$



$t=10s$



$t=15s$



$t=20s$

Generation



$t=0s$



$t=2s$



$t=5s$



$t=10s$



$t=15s$



$t=20s$

Figure 19. Sample of a realistic scene generation based on CARLA conditions.

Ground Truth



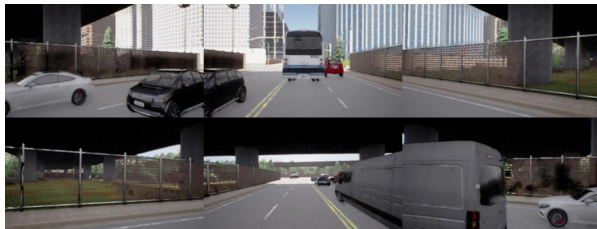
$t=0s$



$t=2s$



$t=5s$



$t=10s$



$t=15s$



$t=20s$

Generation



$t=0s$



$t=2s$



$t=5s$



$t=10s$



$t=15s$



$t=20s$

Figure 20. Sample of a realistic scene generation based on CARLA conditions.